

## ON CENTRIFUGAL SEPARATION OF PARTICLES OF TWO DIFFERENT SIZES

M. UNGARISH and H. P. GREENSPAN†

Department of Mathematics, Massachusetts Institute of Technology, Cambridge, MA 02139,  
U.S.A.

(Received 29 April 1983; in revised form 15 August 1983)

**Abstract**—We consider flow in a centrifugal force field of a non-dilute suspension with particles or droplets of two sizes. The volume fraction and the velocity fields are determined assuming small convection and shear terms. The resulting flow field is quite different from that in a gravitational settling of a similar mixture. In particular, the volume fraction is a function of time and radius in the sectors separated by kinematic shocks and the settling velocity is a non-monotonic function of the particle size.

### 1. INTRODUCTION

We consider the centrifugal separation of a mixture in which the dispersed phase consists of particles (or droplets) of the same density but of two different radii,  $\lambda_1 > \lambda_2$ . The volume fraction of the dispersed phase is taken sufficiently large for particle interactions to be important. The cylindrical container is assumed to be long so that end plate effects can be neglected.

This problem is the extension of two analyses: the exact solution (Greenspan 1983) for a rotating mixture consisting of uniformly sized particles and the gravitational settling of a polydisperse medium considered in Greenspan & Ungarish (1982). However, rotational accelerations introduce some significant new features in the transient process under consideration.

Initially, the homogeneous mixture that occupies the interior of the cylinder is in solid body rotation with the walls at angular velocity  $\Omega^*$ . (This initial state is easily obtained in practice when the spin-up time scale is smaller than that of the separation.) Subsequently, the mixture region is bounded by a sediment layer on one side and a purified fluid on the other (see figure 1). Surfaces of discontinuity, i.e. kinematic shocks, separate the various domains. Another discontinuity develops inside the mixture to divide this region into a sector in which particles of both sizes are present and a second where the component having the larger radial velocity is absent. At time zero, the first sector occupies the whole cylinder but it eventually narrows and disappears. Separation in the second sector of uniformly sized particles is then completed when the shocks labeled 0 and 2 meet.

The mathematical formulation of the problem is given in terms of time or space averaged variables of velocity,  $\mathbf{v}$ , pressure  $p$ , shear stress,  $\tau$  and the volume fraction,  $\alpha$  (Ishii 1975, Delhaye & Achard 1976). Appropriate subscripts, 1, 2,  $C$ ,  $D$  designate variables corresponding to particles of different sizes, the continuous phase and the averaged dispersed phase. For sector (I) (see figure 1), where particles of both sizes are present, we use the equations of motion obtained in Greenspan (1983) ([2.13]–[2.16]) and modified for a coordinate frame rotating with  $\Omega^*$ . For sector (II) the equations [2.1]–[2.6] of Greenspan (1983) can be directly applied.

A main point in the theory of Greenspan is the assumption that interactions in a non-dilute suspension of different sized particles can be described essentially by Stokes' drag law using the local effective viscosity of the mixture

$$\mathbf{M}_k = \kappa \mu_C D(\alpha) \frac{\alpha_k}{\lambda_k^2} (\mathbf{v}_C - \mathbf{v}_k). \quad [1.1]$$

†Consultant, Alfa-Laval AB, Tumba, Sweden.

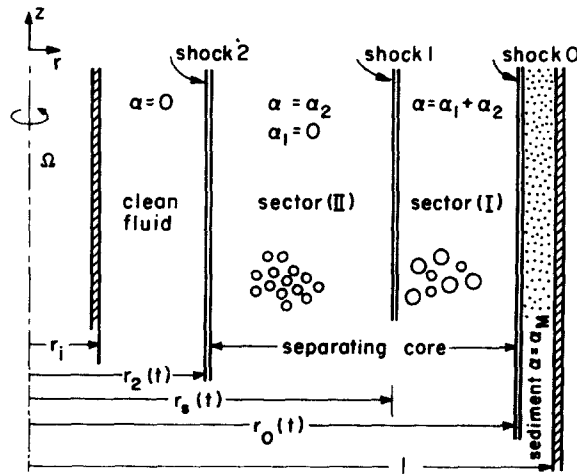


Figure 1. Qualitative description of the flow regions in a long axisymmetric rotating cylinder containing a suspension of heavy particles of two different sizes;  $\alpha$ ,  $\alpha_1$ ,  $\alpha_2$ -volume fractions of dispersed phase, larger and smaller particles.

where  $M_k$  is the drag force per unit volume of mixture acting on the dispersed phase,  $k$ ,  $\mu_c$  is the viscosity of the continuous phase,  $\frac{2}{3} \leq \kappa \leq 1$  is the viscosity ratio in the Hadamard-Rybczynski extension of Stokes' drag and  $\alpha \equiv \alpha_D = \alpha_1 + \alpha_2$  is the volume fraction of the dispersed phase. Furthermore,

$$M_C + M_1 + M_2 = 0. \quad [1.2]$$

The drag correction function used in the present investigation is, as suggested by Ishii & Chawla (1979):

$$D(\alpha) = \left(1 - \frac{\alpha}{\alpha_M}\right)^{-2.5\alpha_M} \quad [1.3]$$

where  $\alpha_M$  is the maximal packing volume of the dispersed phase. However, any form of  $D(\alpha)$  can be incorporated in the subsequent analysis.

Assuming that gravity and the viscous and turbulent stress terms are negligibly small as compared to the Coriolis and the interfacial drag, and that the gradient of the averaged pressure field is the same for all phases, the main dimensionless parameters of the problem are the relative density difference,  $\epsilon$ , the ratio of diameters  $\lambda_2^*/\lambda_1^*$ , and the ratio between the drag and Coriolis forces acting on the larger particle  $\beta = (2/9\kappa)\Omega^*\lambda_1^{*2}/\nu_c^*$  (where  $\nu_c^*$  is the kinematic viscosity of the continuous phase). The present analysis is based on the assumption  $|\epsilon| \ll 1$ .

The value of  $\beta$  may vary considerably in problems of practical interest, so that for  $\nu_c^* = 0.01 \text{ cm}^2/\text{sec}$  (water) and  $\Omega^* = 1000 \text{ sec}^{-1}$ ,  $\beta \simeq 200$  or  $0.02$  for a solid particle of radius 1 mm or 0.01 mm. However, it is important to note that the validity of Stokes' drag becomes questionable when  $\beta$ , which turns out to be a modified Taylor number, is not small. Herron *et al.* (1975) have shown that the Stokes' drag on a single spherical particle in a rotating environment requires corrections of  $O(\sqrt{\beta})$ . Karanfilian & Kotas (1981), who investigated experimentally the motion of a single particle in a centrifuge, found considerable disagreement with Stokes' drag at large Taylor number. However, this deviation, which undoubtedly arises from Taylor-Proudman columns and the tendency of rotating flows to be two-dimensional, is notably affected by the presence of other particles

in a non-dilute suspension. For example, the mean distance between spherical particles is less than two diameters for  $\alpha = 0.1$ . To our knowledge, this is still an uninvestigated matter. Therefore, bearing all this in mind, we shall apply [1.1] without restriction on  $\beta$ . In this regard, the comparison of the results obtained below with simple experiments will perhaps be informative.

## 2. THE FLOW IN THE SEPARATING REGION, SECTOR (I)

We use a cylindrical coordinate system  $(r, \theta, z)$  rotating with angular velocity  $\Omega^*$  around the axis of symmetry,  $z$ , (figure 1) and denote by  $\mathbf{q}_f = u_f \hat{r} + v_f \hat{\theta}$  the velocity of any phase  $f$ . The axial motion is insignificant in the long container under consideration. For centrifugal settling of uniform spherical particles a similarity solution was obtained in Greenspan (1983) where  $\alpha$ ,  $(u_f/r)$  and  $(v_f/r)$  are functions of the time  $t$  only. However, for two or more different particle sizes, it can be shown that such a solution in both sectors (I) and (II) (figure 1) is inconsistent with the continuity conditions across the shock 1. Therefore, we can assume that the similarity still holds in sector (I), but in sector (II) the variables  $\alpha$ ,  $(u_f/r)$ ,  $(v_f/r)$  must depend on  $r$  as well as on  $t$ .

We introduce the following scales for length, velocity, time, density and pressure, respectively:  $r_0^*$  (the outer radius),  $U^* = |\epsilon| \Omega^* r_0^*$ ,  $\tau = r_0^*/U^*$ ,  $\rho_c^*$ ,  $\frac{1}{2} \rho_c^* |\epsilon| (\Omega^* r_0^*)^2$ . In sector (I), velocities are assumed proportional to the radial distance, and the volume fraction is a function of time only

$$\begin{aligned} \alpha_f &= \alpha_f(t); \\ \mathbf{q}_f^* &= U^* r [U_f(t) \hat{r} + V_f(t) \hat{\theta}], \\ p_c^* &= \frac{1}{2} \rho_c^* (\Omega^* r_0^*)^2 r^2 [1 + |\epsilon| P(t)], \end{aligned} \quad [2.1]$$

where

$$\epsilon = \frac{1}{\rho_c^*} (\rho_D^* - \rho_c^*), \quad [2.2]$$

and an asterisk denotes a dimensional variable. The general equations of motion for the fluid and each of  $n$  particle phases as distinguished by diameter are

$$\alpha'_k + 2U_k \alpha_k = 0, \quad [2.3]$$

$$\alpha'_c + 2U_c \alpha_c = 0, \quad [2.4]$$

$$\alpha_c + \alpha = 1, \quad [2.5]$$

$$(1 + \epsilon) [|\epsilon| (U_k' + U_k^2 - V_k^2) - 2V_k] - \frac{\epsilon}{|\epsilon|} = -P + \frac{D(\alpha)}{\beta} \frac{U_c - U_k}{\lambda_k^2}, \quad [2.6]$$

$$(1 + \epsilon) [|\epsilon| (V_k' + 2U_k V_k) + 2U_k] = \frac{D(\alpha)}{\beta} \frac{V_c - V_k}{\lambda_k^2}, \quad [2.7]$$

$$|\epsilon| (U_c' + U_c^2 - V_c^2) - 2V_c = -P - \frac{\alpha}{1 - \alpha} \left( \frac{U_c}{a^2} - \left\langle \frac{U_k}{\lambda_k^2} \right\rangle \right), \quad [2.8]$$

$$|\epsilon|(V'_c + 2U_c V_c) + 2U_c = -\frac{\alpha}{1-\alpha} \frac{D(\alpha)}{\beta} \left( \frac{V_c}{a^2} - \left\langle \frac{V_k}{\lambda_k^2} \right\rangle \right). \quad [2.9]$$

The notation is as follows: prime denotes differentiation in time, and

$$\beta = \frac{2}{9\kappa} \frac{\Omega^* \lambda_1^{*2}}{v_c^*}, \quad [2.10]$$

$$\lambda_k = \frac{\lambda_k^*}{\lambda_1^*}, \quad [2.11]$$

$$\alpha = \alpha_D = \sum_{k=1}^n \alpha_k. \quad [2.12]$$

If  $\phi_k$  is a property of the dispersion associated with the particles of radius  $\lambda_k$  then the global property of the dispersed phase is:

$$\phi_D = \langle \phi_k \rangle = \frac{1}{\alpha} \sum_{k=1}^n \alpha_k \phi_k. \quad [2.13]$$

In particular

$$U_D = \frac{1}{\alpha} \sum_{k=1}^n \alpha_k U_k; \quad V_D = \frac{1}{\alpha} \sum_{k=1}^n \alpha_k V_k; \quad \frac{1}{a^2} = \frac{1}{\alpha} \sum_{k=1}^n \frac{\alpha_k}{\lambda_k^2}. \quad [2.14]$$

(Although we consider only  $k = 1, 2$  the formulation is given for the more general case of  $n$  particle sizes.)

$$U_c = -\frac{1}{1-\alpha} \sum_{k=1}^n \alpha_k U_k = -\frac{\alpha}{1-\alpha} U_D; \quad [2.15]$$

thus, the volumetric flux of the mixture,  $\alpha U_D + (1-\alpha)U_c$  is identically zero. This is a consequence of the similitude expressed by [2.1].

The position of the particle of radius  $\lambda_k$  which was initially at  $r_k(0)$  is

$$r_k(t) = r_k(0) \exp \int_0^t U_k dt. \quad [2.16]$$

Since integration of [2.3] yields

$$\alpha_k(t) = \alpha_k(0) \exp \left( -2 \int_0^t U_k dt \right), \quad [2.17]$$

the particle path is also given as

$$r_k(t) = r_k(0) \frac{\sqrt{\alpha_k(0)}}{\sqrt{\alpha_k(t)}}. \quad [2.18]$$

The positions of particles initially in contact with the inner ( $r = r_i$ ) or outer ( $r = 1$ ) walls are of special importance because they define the locus of the shock boundary separating

sectors (I) and (II) which is then

$$r_s(t) = \begin{cases} \max_k \frac{r_i \sqrt{\alpha_k(0)}}{\sqrt{\alpha_k(t)}}, & \epsilon > 0 \\ \min_k \frac{\sqrt{\alpha_k(0)}}{\sqrt{\alpha_k(t)}}, & \epsilon < 0. \end{cases} \quad [2.19]$$

(We note that sector (II) does not develop if  $\epsilon > 0$  and  $r_i = 0$ .) Multiple shocks occur in the separating core and the velocity of the fastest, shock 1 is

$$\mathcal{U}_1 = \begin{cases} \max_k U_k, & \epsilon > 0 \\ \min_k U_k, & \epsilon < 0. \end{cases} \quad [2.20]$$

The velocity  $\mathcal{U}_0$  of shock labeled 0 in figure 1 which separates the sediment from the mixture is found from the conservation of the volume flux:

$$\sum \alpha_k (U_k - \mathcal{U}_0) = -\alpha_M \mathcal{U}_0. \quad [2.21]$$

In order to determine  $\alpha_k(t)$  and the velocities, [2.3]–[2.9] must be integrated. After some algebra, a standard initial value system of  $(3n + 1)$  equations is obtained (Appendix A). However, some interesting results can be obtained in the limit  $\epsilon \rightarrow 0$ , as follows.

Upon eliminating  $P$  from [2.6] and [2.8] (with  $\epsilon = 0$ ) and substituting in [2.7], a system of equations for the radial velocities is obtained, which by [2.15] may be reduced further to

$$U_k C_{kk} + \sum_{\substack{j=1 \\ j \neq k}}^n C_{kj} U_j = d(\alpha) s \quad [2.22]$$

where

$$s = \frac{\epsilon}{|\epsilon|}; \quad d(\alpha) = \frac{D(\alpha)}{\beta};$$

$$C_{kk} = 4\lambda_k^2 + d^2(\alpha) \left[ \frac{\alpha_k}{1-\alpha} \left( A_k + \frac{1}{\lambda_k^2} \right) + \frac{1}{\lambda_k^2} \right];$$

$$C_{kj} = d^2(\alpha) \frac{\alpha_j}{1-\alpha} \left( A_k + \frac{1}{\lambda_j^2} \right);$$

$$A_k = \frac{\alpha}{1-\alpha} \frac{1}{a^2} + \frac{1}{\lambda_k^2}; \quad \frac{1}{a^2} = \frac{1}{\alpha} \sum_{k=1}^n \frac{\alpha_k}{\lambda_k^2}.$$

Equation [2.7] with  $\epsilon = 0$  becomes:

$$V_c - V_k = \frac{2\beta\lambda_k^2}{D(\alpha)} U_k. \quad [2.23]$$

Equations [2.22]–[2.23] explicitly define the radial velocities and the azimuthal slip velocities as functions of  $\alpha_k(t)$ . The latter variables then emerge from the straightforward

(numerical) integration of [2.3], with the appropriate initial conditions  $\alpha_k(0)$ . (Initial conditions for  $U_k$  cannot be imposed on the system obtained for  $\epsilon = 0$ . The neglected terms  $|\epsilon|U'_k$  are important at short times,  $t \sim |\epsilon|$ , when the velocities adjust to the values which satisfy [2.22]. However  $\alpha_k$  remains essentially unchanged during this short interval.)

Individual expressions for  $V_k$  and  $V_c$  cannot be obtained from the equations with  $\epsilon = 0$  because these variables are essentially governed by nonlinear effects. However, an equation for the mass averaged azimuthal velocity,

$$V_m = \left[ (1 - \alpha)V_c + (1 + \epsilon) \sum_{k=1}^n \alpha_k V_k \right] (1 + \epsilon\alpha)^{-1},$$

in the limit  $\epsilon \rightarrow 0$ , can be obtained with a little algebra:

$$V'_m = \sum_{k=1}^n \alpha'_k (s - 2(V_c - V_k)). \tag{2.24}$$

Consider next the limit of a dilute suspension,  $\alpha_k \rightarrow 0$ . In this case [2.22]–[2.23] become

$$U_k = s \frac{(\beta\lambda_k^2)}{1 + 4(\beta\lambda_k^2)^2} \tag{2.25}$$

$$V_c - V_k = (2\beta\lambda_k^2)U_k = s \frac{2(\beta\lambda_k^2)^2}{1 + 4(\beta\lambda_k^2)^2}. \tag{2.26}$$

For  $s = 1$  (i.e.  $\rho_D^* > \rho_C^*$ ), the dispersed particles are expelled towards the periphery and lag the fluid in the azimuthal direction. Figure 2 shows that these velocities vary considerably with  $(\beta\lambda_k^2)$ , which represents the ratio between the Coriolis and drag forces. No significant relative (slip) motion between the phases is possible when the drag force is large, in which case  $U_k \rightarrow 0$  and  $V_k \rightarrow V_c$  as  $\beta\lambda_k^2 \rightarrow 0$ . On the other hand, when the drag is negligibly small (i.e. large particles,  $(\beta\lambda_k^2) \rightarrow \infty$ ) there is no mechanism to supply the azimuthal acceleration required for a radial motion, and once again  $U_k \rightarrow 0$ . Since  $U_k \rightarrow 0$  in both the small and large particle limits, the radial velocity is not a monotonic function of the size of the particle  $\lambda$ . There is an extremal value of the radial component of velocity corresponding to a particle of radius  $\lambda_{opt}$ . The implication is that small particles may overtake larger particles in the radial direction. (This is expected for  $\beta > 0.5$  but at such large values the theory may be invalid as discussed earlier.)

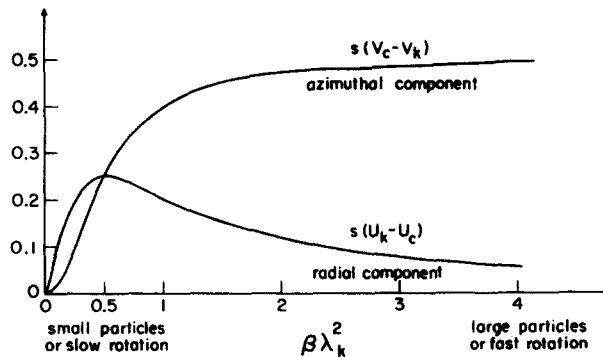


Figure 2. The components of the reduced slip velocity for a dilute suspension vs. ratio between Coriolis and Stokes' forces.  $s = 1$  or  $-1$  for heavy or light particles. Linear ( $\epsilon = 0$ ) solution.

Using [2.24], [2.26] and the initial condition  $V_m(0) = 0$ , we conclude that

$$\begin{aligned} V_m &\approx s[\alpha(t) - \alpha(0)], & \beta &\ll 1 \\ V_m &\approx 0 & , & \beta \gg 1. \end{aligned} \quad [2.27]$$

A considerable backward rotation develops for small  $\beta$  which results from the flux of mass and the conservation of angular momentum.

For moderate values of  $\alpha$  there are some quantitative modifications in the above results which are significant as  $\alpha \rightarrow \alpha_M$ . In certain circumstances, for finite  $\alpha$ , the slower dispersed constituents can be dragged by the continuous phase in a direction opposite to that of  $U_D$  (see [2.15]).

Some numerical examples are given in section 4. The results for the limit  $\epsilon \rightarrow 0$  are compared to the exact solution and good agreement is observed. For particles of only one size, ( $n = 1$ ), the present analysis reduces to that presented in Greenspan (1983).

### 3. THE FLOW IN THE SEPARATING REGION, SECTOR (II)

In the problem under investigation, there are two dispersed components in sector (I), corresponding to the particles of radii  $\lambda_1^*$  and  $\lambda_2^*$ . The slower component  $j$  ( $j = 1$  or  $2$ ) will be left behind in sector (II) by the shock labelled 1 in figure 1, and obviously  $\alpha = \alpha_j$  in this sector.

Using the scaling rules of section 2, the dimensionless variables for velocity and pressure are as follows:  $(u_D, v_D) = r(f, g)$ ;  $(u_C, v_C) = r(F, G)$ ;  $p = r^2(|\epsilon|^{-1} + P)$ . Here  $f, g, F, G$  and  $P$  are functions of  $t$  and  $r$ . It follows that the continuity equations are

$$\frac{\partial \alpha}{\partial t} + \frac{1}{r} \frac{\partial}{\partial r} r^2 \alpha f = 0, \quad [3.1]$$

$$-\frac{\partial \alpha}{\partial t} + \frac{1}{r} \frac{\partial}{\partial r} r^2 (1 - \alpha) F = 0; \quad [3.2]$$

the linear momentum equations are

$$-2g = s - \frac{1}{2r} \frac{\partial}{\partial r} r^2 P + \frac{D(\alpha)}{\beta_j} (F - f); \quad [3.3]$$

$$2f = \frac{D(\alpha)}{\beta_j} (G - g); \quad [3.4]$$

$$-2G = -\frac{1}{2r} \frac{\partial}{\partial r} r^2 P - \frac{\alpha}{1 - \alpha} \frac{D(\alpha)}{\beta_j} (F - f); \quad [3.5]$$

$$2F = \frac{-\alpha}{1 - \alpha} \frac{D(\alpha)}{\beta_j} (G - g); \quad [3.6]$$

where

$$\beta_j = \beta \lambda_j^2 \text{ for } j = 1 \text{ or } 2, \quad [3.7]$$

whichever specie inhabits sector (II). A formula for the volume flux is obtained from [3.1]–[3.2]

$$\alpha f + (1 - \alpha) F = \frac{C(t)}{r^2}. \quad [3.8]$$

Since this flux is continuous across the shock 1, it follows that  $C(t) = 0$  and

$$F = -\frac{\alpha}{1-\alpha}f, \quad [3.9]$$

a result valid for all  $\epsilon$ .

The pressure term may be eliminated from [3.3] and [3.5] to obtain

$$(G - g) = \frac{1}{2} \left\{ s + \frac{D(\alpha)}{\beta_j} \frac{1}{1-\alpha} (F - f) \right\}. \quad [3.10]$$

Upon substituting [3.9]–[3.10] in [3.4] it is found that

$$f = f(r, t) = f(\alpha) = \frac{\frac{D(\alpha)}{\beta_j} s}{4 + \left( \frac{D(\alpha)}{\beta_j} \frac{1}{1-\alpha} \right)^2}. \quad [3.11]$$

The function  $f(\alpha)$ , figure 3, decreases monotonically with  $\alpha$  only for  $\beta_j < 0.7$  but otherwise has a relative maximum. This behavior significantly affects the solution obtained for sector (II).

Equation [3.11] explicitly defines the radial (reduced) velocity in terms of the volume fraction  $\alpha$ . (The same relationship was obtained in [2], but there  $\alpha$  was a function of  $t$  only.) The continuity of the volume flux across shock 1 (whose reduced velocity is  $\mathcal{U}_1$ , see [2.20]) is expressed as

$$\alpha(f(\alpha) - \mathcal{U}_1) = \alpha_j^+(u_j^+ - \mathcal{U}_1) \text{ on } r = r_s(t) \quad [3.12]$$

where  $+$  denotes values in sector (I) and  $r_s(t)$  is the boundary between sectors (I) and (II), figure 1. Since the terms on the r.h.s. are known, [3.12] implicitly defines the boundary condition on  $\alpha$  at  $r = r_s(t)$ , i.e.

$$\alpha = \alpha_s(t) \text{ on } r = r_s(t). \quad [3.13]$$

Recall that  $r_s(t)$  is obtained from the solution in sector (I), see e.g. [2.19].

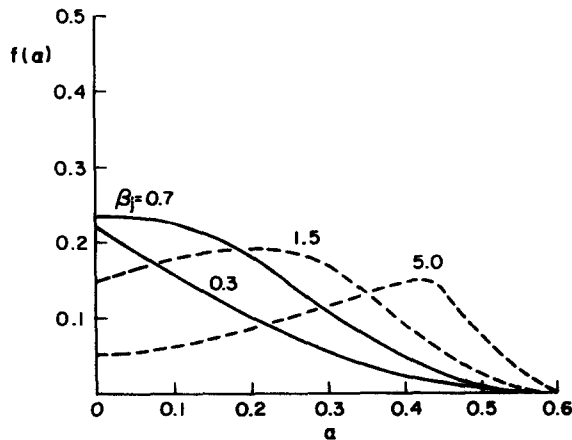


Figure 3. The reduced radial velocity in sector (II) vs volume fraction.  $\beta_j \equiv$  ratio between Coriolis force and Stokes' drag. Linear solution;  $\alpha_M = 0.6$ .



The problem has now been reduced to the task of finding  $\alpha(r, t)$  because the other variables can then be obtained from [3.11], [3.9] and [3.10]. The values of  $\alpha(r, t)$  are obtained as follows.

The substitution of [3.11] into [3.1] yields

$$\frac{\partial \alpha}{\partial t} + \frac{1}{r} \frac{\partial}{\partial r} r^2 \alpha f(\alpha) = 0 \quad [3.14]$$

which can be rewritten as:

$$\frac{\partial \alpha}{\partial t} + \left[ r \frac{d}{d\alpha} \alpha f(\alpha) \right] \frac{\partial \alpha}{\partial r} = -2\alpha f(\alpha). \quad [3.15]$$

This equation can be solved by the method of characteristics, with the initial condition [3.13]. The solution is given in the following parametric form

$$\left. \begin{aligned} r^2 &= \frac{1}{\phi(\alpha)} r_s^2(\gamma) \phi(\alpha_s(\gamma)) & (a) \\ t &= \gamma - \frac{1}{2} \int_{\alpha_s(\gamma)}^{\alpha} \frac{d\alpha}{\phi(\alpha)} = \gamma + \psi(\alpha) - \psi(\alpha_s(\gamma)) & (b) \end{aligned} \right\} [3.16]$$

where

$$\phi(\alpha) = \alpha f(\alpha), \quad \psi(\alpha) = -\frac{1}{2} \int \frac{d\alpha}{\phi(\alpha)} \quad [3.17]$$

and  $\alpha_s(\gamma)$ ,  $r_s(\gamma)$  are the initial values that satisfy [3.13] with the parameter  $\gamma$  replacing the time variable of the shock locus. The shock conditions are satisfied at  $t = \gamma$ , of course.

The value of  $\alpha$  along a characteristic curve emanating from  $\alpha_s(\gamma_1)$  at  $r = r_s(\gamma_1)$ ,  $t = \gamma_1$  is easily calculated but the value of  $\alpha$  for some specific  $t_1$  and  $r_1$  requires a cumbersome iterative search for the appropriate value of  $\gamma$ . Therefore the following approximate procedure may be useful. Denote  $\alpha_0(t)$  and  $\alpha_\gamma(t)$  as the values of  $\alpha$  on the characteristics emanating at  $t = 0$  and  $t = \gamma$ . We anticipate that  $\alpha_\gamma(t) - \alpha_0(t) \sim [\alpha_s(\gamma) - \alpha_0(\gamma)] \equiv \delta(\gamma)$ . This suggests a method of calculation based on the expansion

$$\alpha_\gamma(t) = \alpha_0(t) + \sum_{l=1}^{\infty} [\delta(\gamma)]^l X_l(t), \quad t \geq \gamma \quad [3.18]$$

with

$$X_1 = 1, \quad X_l = 0, \quad l \geq 2 \quad \text{at } t = \gamma. \quad [3.19]$$

For small  $\delta(\ll \alpha_0(\gamma))$ , substitution of [3.18]–[3.19] in [3.16b] and the expansion of  $\psi(\alpha)$  and  $\psi(\alpha_s)$  in Taylor series around  $\alpha_0(t)$  and  $\alpha_0(\gamma)$ , respectively, yields

$$X_1(t) = \frac{\phi(\alpha_0(t))}{\phi(\alpha_0(\gamma))}. \quad [3.20]$$

The similar treatment of [3.16a] shows that on the characteristic emanating at  $t = \gamma$

$$r^2 \cong r_s^2(\gamma) \frac{\phi(\alpha_0(\gamma))}{\phi(\alpha_0(t))}. \quad [3.21]$$

Upon combining these results, we conclude that on a characteristic

$$[\alpha_\gamma(t) - \alpha_0(t)]r^2 \cong [\alpha_s(\gamma) - \alpha_0(\gamma)]r_s^2(\gamma) = \text{const.} \tag{3.22}$$

This solution for  $\alpha$  is invalid when the initial velocity of the characteristic is larger than that of shock 1, i.e.  $f[\alpha_s(\gamma)] + \alpha_s(\gamma)f'(\alpha_s(\gamma)) > \mathcal{U}_1(\gamma)$ , or when characteristics intersect. Although these possibilities cannot be excluded for the whole range of parameters, they will not be considered in the present work.

Since the velocity of shock 2 is that of a dispersed particle, i.e.  $f(\alpha)$ , and the velocity along a characteristic is  $f(\alpha) + \alpha f'(\alpha)$ , this shock is unstable for  $f'(\alpha) > 0$ . This occurs only for larger values of  $\beta$  and moderate  $\alpha$ , (figure 3), in which case an expansion fan is formed instead. In particular, if  $f'(\alpha) > 0$  at  $t = 0$  and  $\epsilon > 0$ , this fan is centered at  $r_i$ . Each ray in this fan satisfies [3.15], and is described by expressions similar to [3.16] but with  $r_s$  replaced by  $r_i$  (the center of the fan) and  $\alpha_s$  replaced by  $\bar{\alpha}$  (which has a value between 0 and  $\alpha_s(0)$ ). The interface is the last characteristic wave in this fan corresponding to  $\bar{\alpha} = 0$ . For small  $\bar{\alpha}$  the solution is approximated by a straightforward series expansion of [3.16] which yields

$$\frac{\alpha}{1 + c\alpha} = \frac{\bar{\alpha}}{1 + c\bar{\alpha}} \exp[-2f(0)t] \quad \text{on} \tag{3.23}$$

$$r = r_i[1 + c(\bar{\alpha} - \alpha)] \exp[f(0)t]$$

where

$$c = f'(0)/f(0).$$

For larger values of  $\bar{\alpha}$  the solution is obtained by numerical integration.

When shock 2 is stable, its position can easily be approximated by using the first term in [3.18] and [3.1] to obtain

$$r_2(t) = r_2(0) \sqrt{\frac{\alpha_0(0)}{\alpha_0(t)}}. \tag{3.24}$$

After the separation of the mixture in sector (I) ( $t > t_1$ ), shock 0 is in direct contact with sector (II) and its velocity is given by the continuity requirement

$$\alpha[f(\alpha) - \mathcal{U}_0] = -\alpha_M \mathcal{U}_0. \tag{3.25}$$

Once again, the approximation  $\alpha \simeq \alpha_0(t)$  yields a simple result, namely

$$r_0 = r_0(t_1) \sqrt{\frac{\alpha_M - \alpha_0(t_1)}{\alpha_M - \alpha_0(t)}} \tag{3.26}$$

where  $r_0(t_1)$  is the position of shock 0 at  $t = t_1$ , obtained from the solution in sector (I).

#### 4. NUMERICAL EXAMPLES

##### Sector (I)

We consider the following illustrative examples

Example	$\lambda_2$	$\beta$	$\alpha_1(0)$	$\alpha_2(0)$
A	0.5	0.1	0.1	0.1
B	0.5	10.0	0.1	0.1
C	0.1	0.1	0.1	0.1

$\lambda_1 = 1$ , of course, and  $s = 1$ .

Some results are presented in figures 4 and 5. Note that in example A,  $U_1 > U_2$ ,  $\alpha_1$  decays faster than  $\alpha_2$ , while the opposite occurs in B where  $U_2 > U_1$ . As  $\alpha \rightarrow 0$  the values  $U_1$  and  $U_2$  predicted by [2.25] are approached, but at the initial stage the discrepancies are large. This reproduces the combination of two effects—the hindering of the particles on each other and the increase of drag with  $\alpha$ —which may increase or decrease the radial velocities according to the parameters of the problem. In particular, the radial velocities increase with time in A and decrease in B.

In example C (not displayed in graphs) it was found that  $U_2$  is negative, which reflects the fact that the small particles are dragged by the continuous phase moving towards the inner wall of the cylinder. However,  $|U_2|$  is smaller than  $|u_0|$ , the velocity of the shock on the sediment, and component 2 settles despite its negative velocity.

The conditions behind the shock 1 are also shown in figures 4–5. It is observed that as volume fraction of the fastest component decays, the shock becomes “weaker”, therefore the corresponding values of the slower component and the velocities as well are almost unaffected across the boundary between sectors (I) and (II). This is expected

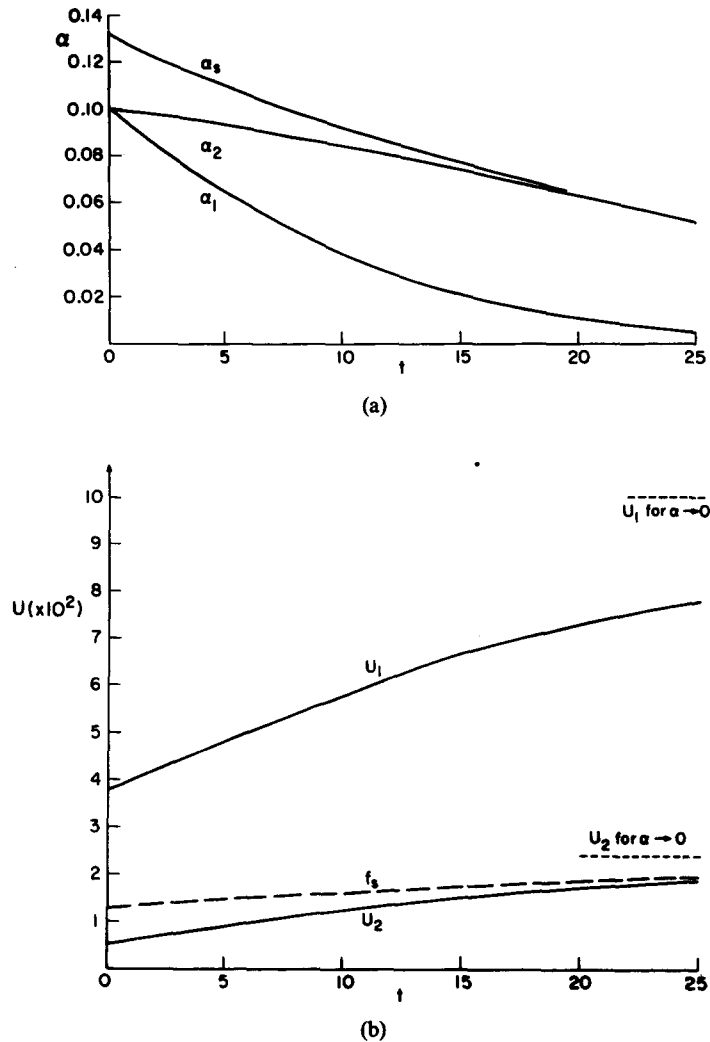
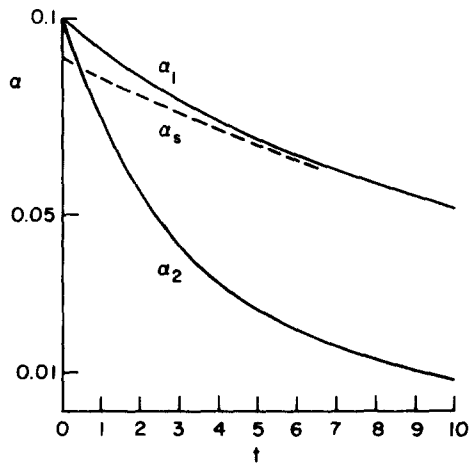
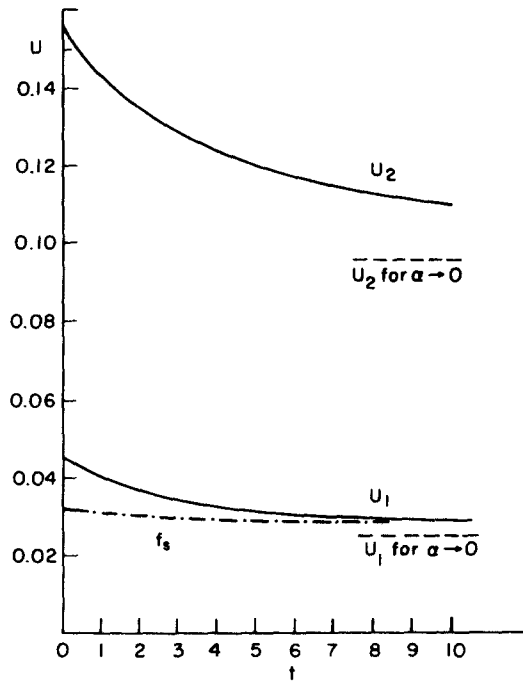


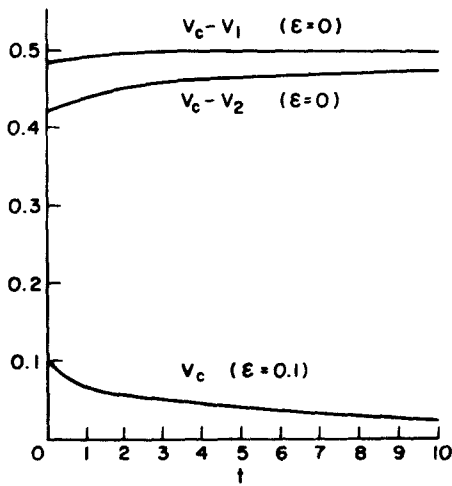
Figure 4. (a) Example A ( $\lambda_2 = 0.5$ ,  $\beta = 0.1$ ,  $s = 1$ ,  $\alpha_M = 0.6$ ). Volume fractions  $\alpha_1$  and  $\alpha_2$  in sector (I) and  $\alpha_s$  behind shock 1 vs time. Linear solution. (b) Example A. Reduced radial velocities,  $U_1$  and  $U_2$  in sector (I) and  $f_s$  behind shock 1 vs time. Linear solution.



(a)



(b)



(c)

Figure 5. (a) Example B ( $\lambda_2 = 0.5$ ,  $\beta = 10$ ,  $s = 1$ ,  $\alpha_M = 0.6$ ). For legend see figure 4(a). (b) Example B. For legend see figure 4(b). (c) Example B. The reduced azimuthal velocities in sector (I) vs time.

because the environments of the particles in sectors (I) and (II) become practically identical. Since  $\beta$  has a dominant influence on the behavior across the shock, the volume fraction and the radial velocity increase in A and decrease in B.

As a check on the linear solution (with  $\epsilon = 0$ ) numerical solutions of the nonlinear system were compiled for  $\epsilon = 0.1$ . Most of these solutions are not shown here. It was found that in example A the agreement between the linear and nonlinear  $\epsilon = 0.1$  results are excellent. In example B,  $U_1$  displays a considerable overshoot (which reaches a value of about 0.35 at  $t \simeq 0.09$ ) in the initial stage but eventually converges toward the linear solution. The reason for this behavior is as follows. The initial conditions  $V_c(0) = V_k(0) = U_k(0) = 0$  used for the nonlinear case give rise to a considerable initial radial acceleration of the dispersed particles, which is a consequence of the unbalanced buoyancy force. Therefore, the heavier particles are thrown towards the periphery and their radial velocity increases. When the drag coefficient is relatively large (case A) the particle cannot develop a considerable radial velocity. But for small drag (case B and especially component 1) a large velocity may be achieved before other forces decelerate the particle. (As an indication of the orders of magnitude involved, we note that balance between buoyancy and drag yields the terminal radial velocity  $U_k = s\beta\lambda_k^2$ , while [2.25] predicts a value which is  $(1 + 4(\beta\lambda_k^2)^2)^{-1}$  times smaller. In cases A, this factor is very close to 1 but in B it attains a value of 401 for the component 1.) However, this overshoot decays so rapidly that its influence on the behavior of  $\alpha$  is not substantial. The values of  $\alpha$  for linear and nonlinear solutions in examples A and B are in very good agreement. The azimuthal velocities of example B are shown in figure 5(c). The agreement of the linear case with the exact  $\epsilon = 0.1$  solution is very good for  $t > 1$  (the latter displays some oscillation for a short period). It is seen that  $V_c$  has a small positive value, while the dispersed phase lags considerably behind. In example A, it was found that the azimuthal slip velocities are very small, but a considerable backward rotation of the core is developed (e.g. at  $t = 20$ ,  $V_1 = -0.134$ ,  $V_2 = -0.122$ ,  $V_c = -0.122$ ) because of the loss of angular momentum of the expelled dispersed particles, which is also transferred to the continuous phase through the large drag interaction. These results are in fair agreement with [2.26].

### Sector (II)

The solution in this sector for examples A and B, with  $r_i = 0.5$ , was calculated and some results are presented in figures 6 and 7. Figures 6(a) and 7(a) show the projection of the sectors in the  $r, t$  plane. It is observed that the first characteristic propagates considerably slower than shock 2 in example A and faster in B. Therefore an expansion fan is formed in the latter case. In example A,  $\alpha_j$  decreases in the radial direction in sector II and then decreases again across shock 1, while the opposite occurs in example B. The radial variation becomes weaker as  $\alpha_j$  decreases. Comparison of the exact solution [3.16] to the approximation [3.18] indicates good agreement. In particular, the value of  $[\alpha(t) - \alpha_0(t)]r^2$  was found to be constant (within about 2% of deviation) along the characteristics of examples A and B, as predicted by [3.22].

## 5. CONCLUDING REMARKS

We have considered the centrifugal separation of a mixture in which the dispersed phase consists of particles (or droplets) of the same density but of two different radii,  $\lambda_1^* > \lambda_2^*$ . The assumptions that the cylindrical container is sufficiently long for end effects to be negligible and that the relative density difference between the phases,  $\epsilon$ , is small, are valid for many potential applications. The volume fraction, the velocities, and the position of the kinematic shocks in this time dependent process were calculated for illustrative parameter values. The flow of the "purified" constituents is essentially similar to that discussed in Greenspan (1983).

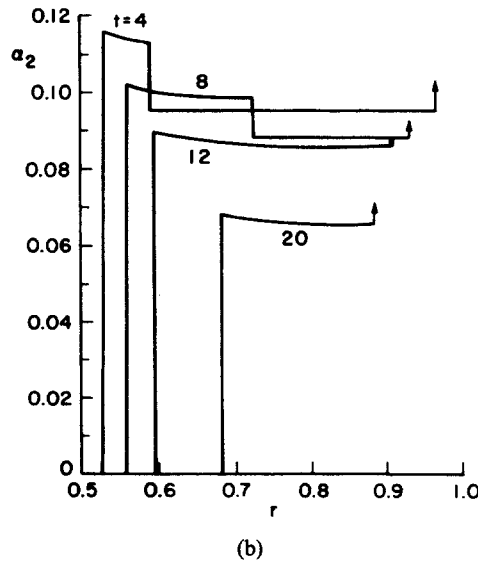
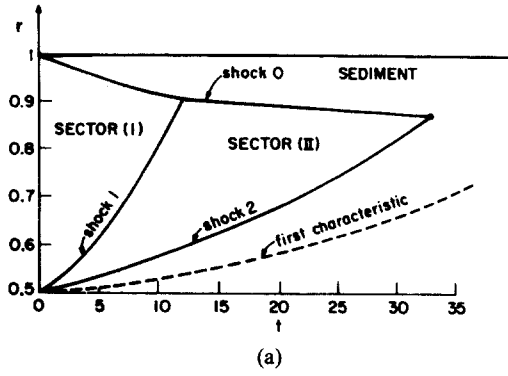


Figure 6. (a) Example A. Trajectories of kinematic shocks and of the first characteristic and evolution of the separation zones in a container with  $r_i = 0.5$ . (b) Example A. The volume fraction of the slower constituent vs radius at different times in a container with  $r_i = 0.5$ . The arrow indicates the jump into sediment layer.

The motion is quite different from that in the gravitational settling of a similar mixture, because the volume fraction  $\alpha$  is here a function of  $t$  and  $r$  while in the latter case  $\alpha$  is usually constant between kinematic shocks. Another interesting result is that the settling velocity is not a monotonic function of the particle size. However, this feature may be

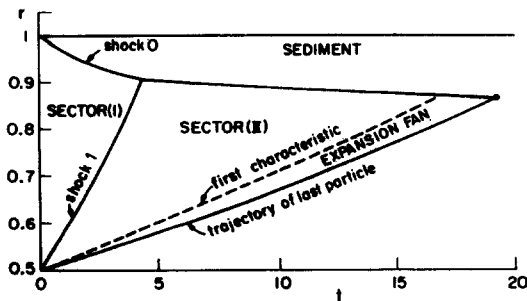


Figure 7(a).

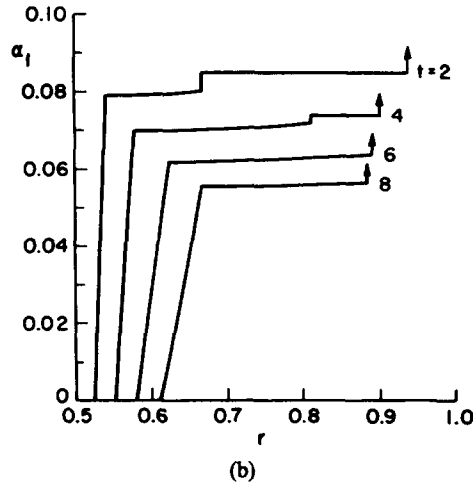


Figure 7. (a) Example B. For legend, see figure 6(a). (b) Example B. For legend, see figure 6(b).

illusory since it requires a fairly large value of the parameter  $\beta$  when strong local rotational effects (i.e. formation of Taylor columns) considerably influence the drag force. On the other hand, the small interparticulate distance in a non-dilute suspension may be a compensating factor. In this regard, the comparison of the present results with simple experiments will perhaps be informative.

*Acknowledgement*—This work was supported in part by a Bantrell Fellowship awarded to the first author and by the National Science Foundation under Grant MCS-8213987.

#### REFERENCES

- DELHAYE, J. M. & ACHARD, J. L. 1976 On the averaging operators introduced in two-phase flow modeling. *Spec. Meet. Transient Two-phase Flow*, Toronto.
- GREENSPAN, H. P. 1983 On centrifugal separation of a mixture. *J. Fluid Mech.* **127**, 91–101.
- GREENSPAN, H. P. & UNGARISH, M. 1982 On hindered settling of particles of different sizes. *Int. J. Multiphase Flow* **8**, 587–604.
- HERRON, I. H., DAVIS, H. & BRETHERTON, F. P. 1975 On the sedimentation of a sphere in a centrifuge. *J. Fluid Mech.* **68**, 209–234.
- ISHII, M. & CHAWLA, T. C. 1979 Local drag in dispersed two-phase flow. *Argonne National Laboratory*, 79–105.
- ISHII, M. 1975 *Thermo-Fluid Dynamic Theory of Two-Phase Flow*. Eyrolles.
- KARANFILIAN, S. K. & KOTAS, T. J. 1981 Motion of a spherical particle in a liquid rotating as a solid body. *Proc. R. Soc. London, Ser. A* **376**, 525–544.

#### APPENDIX A

The solution of the system [2.3]–[2.9] for finite  $\epsilon$  is obtained in the following way. Elimination of  $P$  from [2.6] and [2.8] gives

$$(1 + \epsilon)[\epsilon|(U'_c + U_k^2 - V_k^2) - 2V_k] - s - [\epsilon|(U'_c + U_c^2 - V_c^2) - 2V_c] \\ = \frac{D(\alpha) U_c - U_k}{\beta} \frac{U_c - U_k}{\lambda_k^2} + \frac{\alpha}{1 - \alpha} \left( \frac{U_c}{a^2} - \left\langle \frac{U_k}{\lambda_k^2} \right\rangle \right) \quad [A1]$$

Using [2.12]–[2.13] and [2.3]–[2.5], we obtain

$$U_C = -\frac{1}{1-\alpha} \sum_{k=1}^n \alpha_k U_k, \quad [\text{A2}]$$

and

$$U'_C = 2U_C^2 + 2\frac{1}{1-\alpha} \sum_{k=1}^n \alpha_k U_k^2 - \frac{1}{1-\alpha} \sum_{k=1}^n \alpha_k U'_k. \quad [\text{A3}]$$

Substitution of [A3] in [A1] and rearrangement yields

$$\begin{aligned} & \left(1 + \epsilon + \frac{\alpha_k}{1-\alpha}\right) U'_k + \frac{1}{1-\alpha} \sum_{\substack{j=1 \\ j \neq k}}^n \alpha_j U'_j \\ &= \frac{1}{|\epsilon|} \{ \text{RHS(A1)} + 2[(1+\epsilon)V_k - V_C] + s \}, \\ & -(1+\epsilon)(U_k^2 - V_k^2) + 3U_C^2 - V_C^2 + 2\frac{1}{1-\alpha} \sum_{k=1}^n \alpha_k U_k^2. \quad [\text{A4}] \end{aligned}$$

Equation [4] explicitly defines  $U'_k$  in terms of the other variables. Explicit equations for  $V'_k$  and  $V_C$  are easily obtained from [2.7] and [2.9], and equations for  $\alpha'_k$  are given by [2.3]. Thus, a standard system of ordinary differential equations for  $(U_k, \alpha_k, V_k, V_C)$ ,  $1 \leq k \leq n$ , is obtained.